

PNAS

www.pnas.org

Supplementary Information for

POT1-TPP1 differentially regulates telomerase via POT1 His266 as a function of telomere ssDNA length
Mengyuan Xu^a, Janna Kiselar^b, Tawna L. Whited^a, Wilnelly Hernandez-Sanchez^a, & Derek J. Taylor^{a,c,1}
¹correspondence to derek.taylor@case.edu

This PDF file includes:

Supplementary text
Figs. S1 to S9
Tables S1 to S4
References for SI reference citations

Supplementary Information

Material and Methods

Protein expression and purification

The N-terminal GST-tagged POT1-N (1-340) fusion construct was expressed using the recombinant baculovirus expression system to infect *Spodoptera frugiperda* 9 (Sf9) insect cells as described previously (1). After 72 h infection, cells were pelleted and stored at -80°C . Frozen cell pellets were resuspended in lysis buffer containing 25 mM Hepes (pH 8.0), 200 mM NaCl, 100 mM $\text{Na}_2\text{HPO}_4/\text{NaH}_2\text{PO}_4$ (pH 8.0), 5 mM DTT, 5 mM benzamidine, 1 mM PMSF, and 1 cOmplete ULTRA protease inhibitor cocktail tablet (Roche). Cells were then lysed using sonication and incubated with 2 units/mL of RQ1 DNase I (Promega) for 30 min before removal of cellular debris by ultracentrifugation at 36K rpm for 1 hour at 4°C . Following ultracentrifugation, supernatant was applied to a gravity filtration column with buffer washed GST-beads (Invitrogen). Bead binding was performed at 4°C , then rinsed with wash buffer containing 25 mM Hepes (pH 8.0), 150 mM NaCl and 50 mM $\text{Na}_2\text{HPO}_4/\text{NaH}_2\text{PO}_4$ (pH 8.0). Protein was eluted with wash buffer containing 15 mM glutathione. PreScission protease (GE Healthcare) was then added to remove the N-terminal GST tag followed by size-exclusion chromatography (SEC) using a Superdex 200 HiLoad 16/60 chromatography column on an AKTA Purifier10 FPLC system (GE Healthcare). Protein fractions were pooled, concentrated with a Millipore Amicon Ultra 10K centrifugal column to 1 mg/mL and stored at -80°C . Full-length POT1 (1-634) with an N-terminal GST-tag and N-terminal 6 \times His-tagged TPP1 (89-334) proteins were co-expressed and co-purified following a strategy similar to that described above for POT1-N, including affinity purification, followed by GST-tag removal and SEC purification.

DNA oligonucleotides and 5' end-labeling

The hT12 (5'-GGTTAGGGTTAG-3' and 5'-TTAGGGTTAGGG-3') and hT72 (5'-(GGTTAG)₁₂-3') oligonucleotides were synthesized by IDT. 5' end-labeling was performed using 25 pmols of oligonucleotide reacted with radiolabeled ATP[γ - ^{32}P] (Perkin Elmer) and T4 Polynucleotide Kinase (New England BioLabs) as previously described (2). Labeled products were purified from unreacted nucleotide using illustra MicroSpin G-25 columns (GE Healthcare).

Stoichiometric gel shift assay

Stoichiometric gel shift assays were performed to evaluate loading of POT1-TPP1 proteins on hT12 and hT72 telomere ssDNA substrates. Each 10 μL reaction contained 0.2 μM ssDNA with approximately 4% of it being 5' end ^{32}P labeled. POT1-TPP1 was added to each reaction at 0, 0.2, 0.4, 0.8 μM for hT12, and 0, 0.3, 0.6, 0.9, 1.2, 2.4, 3.6, and 4.8 μM for hT72 to reach the molar ratios indicated. Reactions were conducted in buffer containing 60 mM Hepes (pH 8.0), 75 mM NaCl, 5 mM DTT, 5 $\mu\text{g}/\text{mL}$ BSA, 1.2 $\mu\text{g}/\text{mL}$ tRNA and 6.25% glycerol. After 30 minutes of incubation on ice, reactions were loaded onto 4–20% Tris-borate non-denaturing gel (Invitrogen) and run at 125 V for 1 hour and 20 minutes. Gels were then dried, and scanned for densitometry using a Typhoon FLA 9500 biomolecular imager (GE Healthcare).

Assembly of protein-ssDNA complexes as monomer and hexameric complexes

POT1-TPP1 protein was assembled with hT12 or hT72 ssDNA to form monomeric or hexameric species of nucleoprotein complexes. SEC was used to separate protein-ssDNA complex from unbound ssDNA. For PT-hT12 complex, hT12 was incubated with POT1-TPP1 in three-times molar excess to ensure that all POT1-TPP1 protein was in complex with hT12 ssDNA. PT-hT12 was then separated from unbound hT12 ssDNA by SEC. Conversely, for PT-hT72 complexes, hT72 ssDNA was incubated with 18-times molar excess of POT1-TPP1 protein to saturate the hT72 ssDNA. The PT-hT72 hexamer was then separated from free POT1-TPP1 protein using SEC. Protein-ssDNA complex fractions were pooled and concentrated with a Millipore Amicon Ultra 10K centrifugal column to ~5 μ M. Complex assembled from POT1-N protein (POT1-N-hT12 and POT1-N-hT72) were assembled using a similar strategy.

Synchrotron radiolysis and POT1 proteolysis using pepsin

Radiolysis experiments were performed at beamlines X28C and 5.3.1 of the National Synchrotron Light Source at Brookhaven National Laboratory and Advanced Light Source at Lawrence Berkeley National Laboratory. The X-ray beam parameters were optimized by using Alexa-488 fluorophore assay. All samples were exposed for 0-20 milliseconds (X28C) and for 0-800 μ s (5.3.1) at ambient temperature and immediately quenched with methionine amide at the 10mM final concentration to prevent secondary oxidation (3). All protein samples were then reduced with 10 mM dithiothreitol (DTT) at 56°C for 45 minutes and alkylated with 25 mM iodoacetamide at room temperature and in the dark for 45 minutes. Prior to digestion, formic acid (FA) was added to all samples at a final concentration of 0.5% to achieve a pH between 1 and 2. Protein samples were digested with pepsin (Promega, Madison, WI) at 37°C for 3 h with an enzyme:protein molar ratio of 1:10. The digestion reaction was terminated by heating samples at 95°C for 2 minutes.

LC-MS Analysis

Liquid chromatography mass spectrometry (LC-MS) analysis of digested samples for hydroxyl radical footprinting experiments were performed using an Orbitrap Elite mass spectrometer (Thermo Electron, San Jose, CA) interfaced with a Waters nanoAcquity UPLC system (Waters, Taunton, MA). Proteolytic peptides were desalted on a trap column (180 μ m \times 20 mm packed with C18 Symmetry, 5 μ m, 100 Å (Waters, Taunton, MA)) and subsequently eluted on a reverse phase column (75 μ m \times 250 mm nano column, packed with C18 BEH130, 1.7 μ m, 130 Å (Waters, Taunton, MA)) using a gradient of 2 to 42% mobile phase B (100% acetonitrile/0.1% formic acid) vs. mobile phase A (100% water/0.1 % formic acid) over a period of 60 minutes at 37°C with a flow rate of 300 nl/min. A total of 250 ng of proteolytic peptides were loaded on column for each MS analysis. Peptides eluting from the column were introduced into the nano-electrospray source at a capillary voltage of 2.5 kV. All MS data were acquired in the positive ion mode. For MS1 analysis, a full scan was recorded for eluted peptides (m/z range of 360–1600) in the Orbitrap mass analyzer with resolution of 120,000 followed by MS/MS of the 20 most intense peptide ions scanned in the ion trap mass analyzer. Selected ion currents for modified and unmodified peptic peptides in MS1 experiments were used to determine the extent of oxidation for each modified site. In HRF experiments, the resulting MS/MS data were searched against a POT-N or POT1 and TPP1 sequence database using Mass Matrix software to identify sites of modification. In particular, MS/MS spectra were searched for nonspecific peptides from POT1 and TPP1 protein sequences using mass accuracy values of 10 ppm and 0.7 Daltons for MS1 and MS2 scans respectively, with allowed variable modifications including carbamidomethylation for cysteines and all known oxidative modifications

previously documented for amino acid side chains. In addition, MS/MS spectra for each site of proposed modification were manually examined and verified.

Modification rate calculation for a specific site

The integrated peak areas of the unmodified peptide (A_u), and of a peptide in which a residue is modified (A_m) derived from selected ion chromatograms, were used to calculate the fraction unmodified for each specific modified species according to the formula: $F_u = 1 - (A_m / (A_u + \sum A_m))$, where $\sum A_m$ is the sum of all modified products for a particular peptide. Dose-response curves generated using unmodified fraction for each specific site of modification plotted versus X-ray exposure time. The fraction unmodified for each site of modification was fit to the equation $F_u(t) = F_u(0)e^{-kt}$, where $F_u(0)$ and $F_u(t)$ are the fraction of unmodified at time 0 and time t, respectively, and k is a first order rate constant. The peptide segments and the amino acid side chains in each segment for which rates were determined are provided in Table S1. A modification rates ratio comparing protein-only state (POT1-N) versus protein bound to short telomere ssDNA hT12 (POT1-N-hT12) was calculated by dividing the modification rate for each modified site derived from POT1-N protein samples by the modification rate for the same sites of modification derived from POT1-N-hT12. Similarly, the modification ratio comparing protein bound to hT12 (POT1-N-hT12) versus hT72 (POT1-N-hT72) was the quotient of modification rate of each modified site from POT1-N-hT12 sample against the modification rate of the same site from POT1-N-hT72 sample. For the residues identified from multiple peptides, the average values were used.

The reported values were depicted as modification rate ratios following normalization as described previously (4). Briefly, the mean and median modification rate ratios were determined in \log_{10} scale and averaged to provide a normalization factor used for individual data points. Normalized modification rate ratios were calculated by subtracting the normalization factor from the measured modification rate ratio for the same residue under different experimental conditions. The normalization in log scale is inspired by the geometric mean, which computes the arithmetic mean of a set of the logarithm transformed values (5). Also, the normalization factor was calculated by averaging the mean and median values to better represent the data compiled. Normalized ratios and normalization factors were converted back to linear scale for presentation in Table S2. Normalized modification ratios of POT1-TPP1 samples were calculated following the same strategy as POT1-N samples (Table S3 and S4).

Electrophoretic mobility shift assays (EMSAs)

Protein-DNA binding reactions were performed in buffer containing 60 mM HEPES (pH 8.0), 75 mM NaCl, 5 mM DTT, 5 $\mu\text{g}/\text{mL}$ BSA, 1.2 $\mu\text{g}/\text{mL}$ tRNA and 6.25% glycerol. Reactions were performed using 50 pM ^{32}P -labeled DNA (hT12, hT72) or 4 nM IRD700 fluorescent dye labeled DNA (a3, a5) and variable concentrations of recombinant POT1-TPP1 protein. For hT12, wild type and Y36N mutant POT1-TPP1 were performed under the concentration range of 0 to 500 nM, while H266L mutant POT1-TPP1 concentrations ranged from 0 to 10 μM . For hT72 binding reactions, both wild type and mutant (Y36N or H266L) POT1-TPP1 proteins were used at concentrations ranging from 0 to 1 μM . Binding reactions were incubated for 15 min at room temperature before 8 μL of the reaction was loaded onto a 5% Tris-borate non-denaturing gels (Invitrogen). Gels were run at 125 V for 30 min for hT12 and 55 min for hT72 ssDNA. Gels were dried and scanned using a Typhoon FLA 9500 biomolecular imager (GE Healthcare) and densitometry was performed using ImageQuant TL 1D v8.1 software (GE Healthcare). For hT12, a3, and a5, the

quadratic equation was used to fit and obtain equilibrium dissociation constants (K_D) for each construct. For hT72, the highest molecular weight band representing six-proteins bound was quantified against the bottom band representing free DNA. The fraction of saturated complex was plotted against POT1-TPP1 protein concentration and subsequently fitted using the Hill equation with Origin8.0 software. Fitting was performed by allowing all parameters to float to obtain the best fit for apparent dissociation constants (K_{app}) for each construct. In doing so, Hill coefficients were determined to be $n = 3.9 \pm 0.1$, 2.9 ± 0.3 , and 2.5 ± 0.2 for wild type, Y36N, and H266L constructs, respectively. Reported values represent the average dissociation constants, with calculated standard errors, derived from three independent experiments for each condition.

Size-exclusion chromatography analysis

Size-exclusion chromatography analyses were performed using a Superdex 75 column (increase 3.2/300, bed volume 2.4 mL) (GE Healthcare Life Sciences) on a Shimadzu HPLC system in buffer containing 25 mM Hepes (pH 8.0) and 150 mM NaCl. POT1-TPP1 wildtype or H266L mutant (10 μ M) was incubated with or without (TTAGGG)₂ ssDNA (20 μ M) for 30 min on ice, then loaded onto the column. The SEC profile was calibrated using gel-filtration protein standards (Bio-Rad). Molecular weight (Log_{10}) of standards were plotted against the ratio of V_e/V_o elution volumes (where V_e is the elution volume for each standard and V_o is the void volume). The standard masses were fit using the equation $\text{Log}_{10}(\text{Molecular weight}) = -1.7135 * V_e/V_o + 7.2454$ and sample molecular weights were determined by fitting to the data.

Multi-angle light scattering (MALS) analysis

MALS determines the molecular weight of molecules via a method that is independent of molecular mass reference standards, column calibration and assumptions of molecular shape (6). In addition, SEC-MALS separates mixtures of oligomers and measures the absolute molecular weight of an oligomer in elution fractions. Multi-angle light scattering (MALS) experiments were performed immediately following size-exclusion chromatography (SEC) by online measurement of static light scattering (mini DAWN TREOS, Wyatt Technology), differential refractive index (dRI, Optilab rEX, Wyatt Technology) at a wavelength of 658 nm and ultraviolet absorbance at a wavelength of 280 nm (Dionex ultimate 3000 variable wavelength detector). For this assay, a ProSEC 300S, 300 x 7.5 mm SEC column was connected upstream of the MALS-RI detectors and used to fractionate the injected sample. The SEC-MALS-RI system as a whole was validated using BSA (Sigma-Aldrich). Prior to sample injection (40 μ L), the column was equilibrated at a flow rate of 0.3 mL/min in 50 mM HEPES pH 7.5, 150 mM NaCl. The chromatogram and resultant molecular weight data were analyzed using the Astra 5.3 software from Wyatt Corporation.

Direct telomerase incorporation assay

Telomerase activity assays were performed by mixing 2 μ L of hTR and hTERT transfected HEK 293T cell lysate into a 15 μ L reaction mixture containing 35 mM Tris-HCl pH 8.0, 0.7 mM MgCl₂, 1.8 mM β -mercaptoethanol, 0.7 mM spermidine, 35 mM KCl, 500 μ M dTTP, 500 μ M dATP, 2.9 μ M dGTP, 2 μ L [α -³²P]-dGTP (10 μ Ci/ μ L, 3000 Ci/mmol, Perkin-Elmer) and 0.1 μ M hT12 or hT72 primer. Five microliters of purified POT1-TPP1 (wild type, Y36N and H266L) protein complexes (at 0.8 μ M or 4.8 μ M) were added to reach the final concentration of 0.2 μ M for hT12 or 0.2 μ M and 1.2 μ M for hT72. For reactions without POT1-TPP1 protein, an equivalent volume of the appropriate

protein buffer was used instead. The telomerase reaction was carried out for 30 min at 30°C and then quenched by adding 100 µL of 3.6 M NH₄OAc, 20 µg of glycogen, 4 µL of 10 mM EDTA. A 5'-³²P-labeled 12 nt, 15 nt, or 53 nt oligo was used as loading control. The radioactivity of the loading control was determined by liquid scintillation counting and 400 cpm were loaded into each reaction mixture. All ssDNA products synthesized in the assay were ethanol-precipitated and analyzed on a 12% polyacrylamide/7 M urea/1× TBE denaturing gel. Gels were dried and subjected to densitometry results that were digitized with a Typhoon FLA 9500 biomolecular imager (GE Healthcare) and quantified using ImageQuant TL 1D v8.1 software (GE Healthcare).

Quantification of telomerase assay products was performed as described previously (7, 8). Briefly, relative intensities for each hexamer repeat were determined and normalized against the loading control for each lane. Total activity is reported as total lane counts by summing the relative intensities of all normalized bands within a lane. Repeat addition processivity was calculated by first correcting for the number of radiolabeled Gs incorporated within each hexamer repeat and then calculating the fraction left behind (FLB) by subtracting and dividing the sum of intensities for each round of extension (1-n) by the entire sum of intensities for the total lane count. The ln (1-FLB) was plotted against the repeat number of telomerase extension and the slope was fitted to the linear portion of those data. Repeat addition processivity was defined as $-0.693/\text{slope}$.

Stopped-flow circular dichroism

The kinetics of G-quadruplex destabilization of hT72 ssDNA was monitored upon rapid mixing of ssDNA with POT1-TPP1 protein. hT72 oligonucleotides were first prepared by heating at 95 °C for 5 min followed by slow cooling to room temperature. 200 nM of hT72 and 2.4 µM of POT1-TPP1 (either wild type or H266L mutant), all prepared in 60 mM HEPES (pH 8.0) and 75 mM NaCl buffer, were mixed using the stopped-flow device equipped on a PiStar 180 spectrophotometer (Applied Photophysics). Circular dichroism was conducted at 25°C with signal changes monitored at 295nm (path length 1 cm, bandwidth 4 nm) over time for 300s at a rate of three measurements per second. Data were fitted to a double exponential equation: $CD_{295} = A_1 \exp^{-k_{obs1}t} + A_2 \exp^{-k_{obs2}t} + c$, where k_{obs1} and k_{obs2} represent the two independent rates used for fitting the data.

CRISPR-Cas9 editing cell lines and telomere restriction fragment (TRF) assay

The genome of HCT116 cells were edited using CRISPR-Cas9 techniques by Washington University's Genome Engineering and iPSC Center (GEIC) as previously described (9). The cells were transfected with sgRNA sequence (TTAGAGTTTCATCTTCATGGNGG) (Addgene #43860) and Cas9 pDNA (Addgene #43945) via nucleofection (Lonza 4D-Nucleofector, X Unit). The edited cells were validated by next-generation sequencing (NGS) and Sanger sequencing. Parental and H266L mutated HCT116 cells were grown in Dulbecco's Modified Eagle Medium (DMEM) supplemented with 10% fetal bovine serum (FBS) at 37°C with 5% CO₂ for 78 population doublings (PDs). 5×10⁶ cells were harvested at 0, 28, 55, 78 population doublings and genomic DNA were isolated (Sigma-Aldrich, Catalog# NA2110). TRF analysis was performed using a commercial kit (TeloTAGGG Telomere Length Assay, Catalog# 12209136001, Roche Diagnostics Corporation, Indianapolis, IN, USA). A total of 2 µg DNA was digested overnight with Rsa I and Hinf I at 37°C and electrophoresed through 0.5% agarose gels in 1×TBE at 5 V/cm for 6 hrs. Gels were denatured and neutralized prior to capillary transfer overnight. Telomere DNA was transferred onto a HybondTM- N+ membrane (GE Healthcare) using 20× SSC buffer. The transferred DNA was fixed

by UV crosslinking. The cross-linked membrane was then hybridized with DIG-labeled telomere probes with the sequence (TTAGGG)₄ overnight at 42°C. After hybridization, the membrane was washed with buffer 1 (2× SSC, 0.1% SDS) at room temperature for 15 min and then washed twice with buffer 2 (0.5× SSC, 0.1% SDS) at 55°C for 15 min. Then, the membrane was incubated with Anti-DIG-AP antibody. Finally, the membrane was incubated with CDP-Star solution (Roche) for detection and imaged with ODYSSEY imaging system (LI-COR). Image quantification was performed using Image Studio software to measure the intensity value of each telomere smear. The weighted telomere length mean was determined by dividing each lane into 60 boxes and applying the formula $\Sigma ODi/\Sigma(ODi/Li)$, where ODi is the intensity of box i and Li corresponds to the length of the DNA in box i as determined using DNA markers and a standard curve (10).

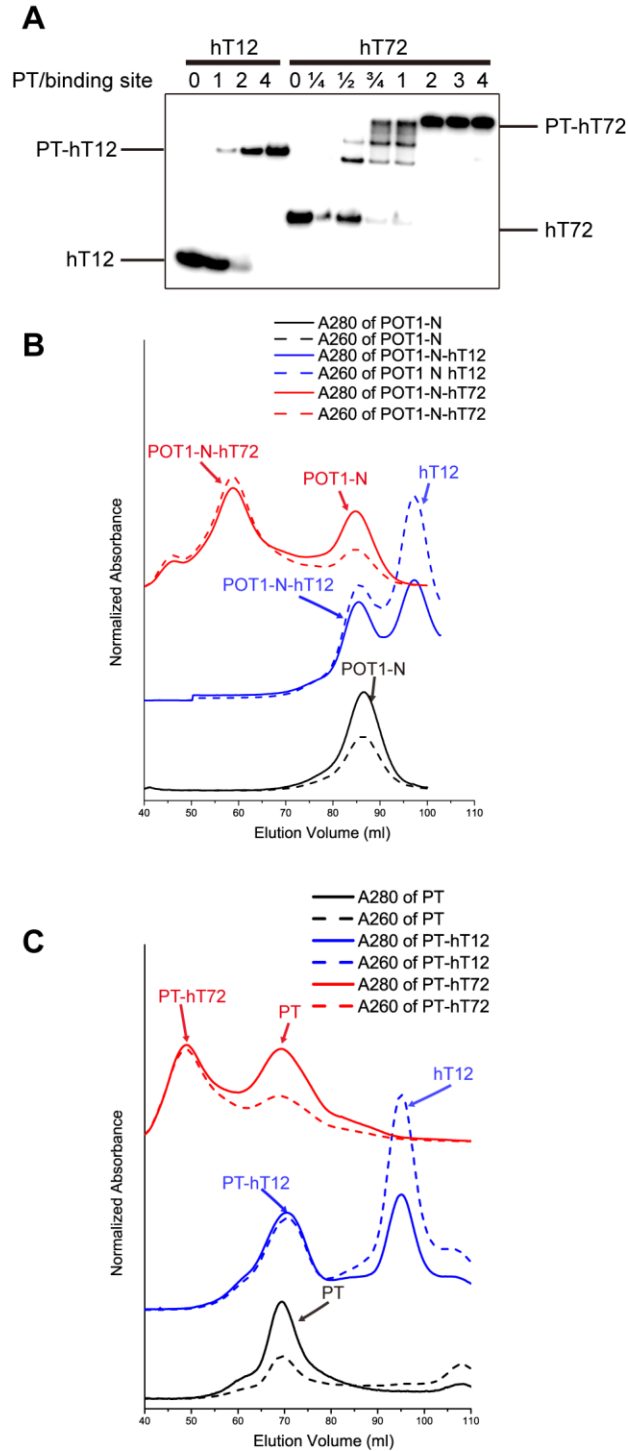


Figure S1. POT1-N and POT1-TPP1 coat long telomere ssDNA substrates. **A.** Electrophoretic mobility shift assays under stoichiometric conditions of POT1-TPP1 coating different lengths of telomere ssDNA substrates. Molar ratios of POT1-TPP1 proteins to the number of binding sites in each oligo are indicated on the top of the gel. **B.** Size-exclusion chromatography of POT1-N with or without telomere ssDNA substrates. Profiles of the POT1-N, POT1-N-hT12, and POT1-N-hT72 complex are shown in black, blue, and red, respectively. Absorbance at 280nm is shown as solid lines and the absorbance at 260nm is shown as dashed lines. **C.** Size-exclusion chromatograms of POT1-TPP1 with or without telomere ssDNA substrates. Label coloring schemes are the same as in panel **B.**

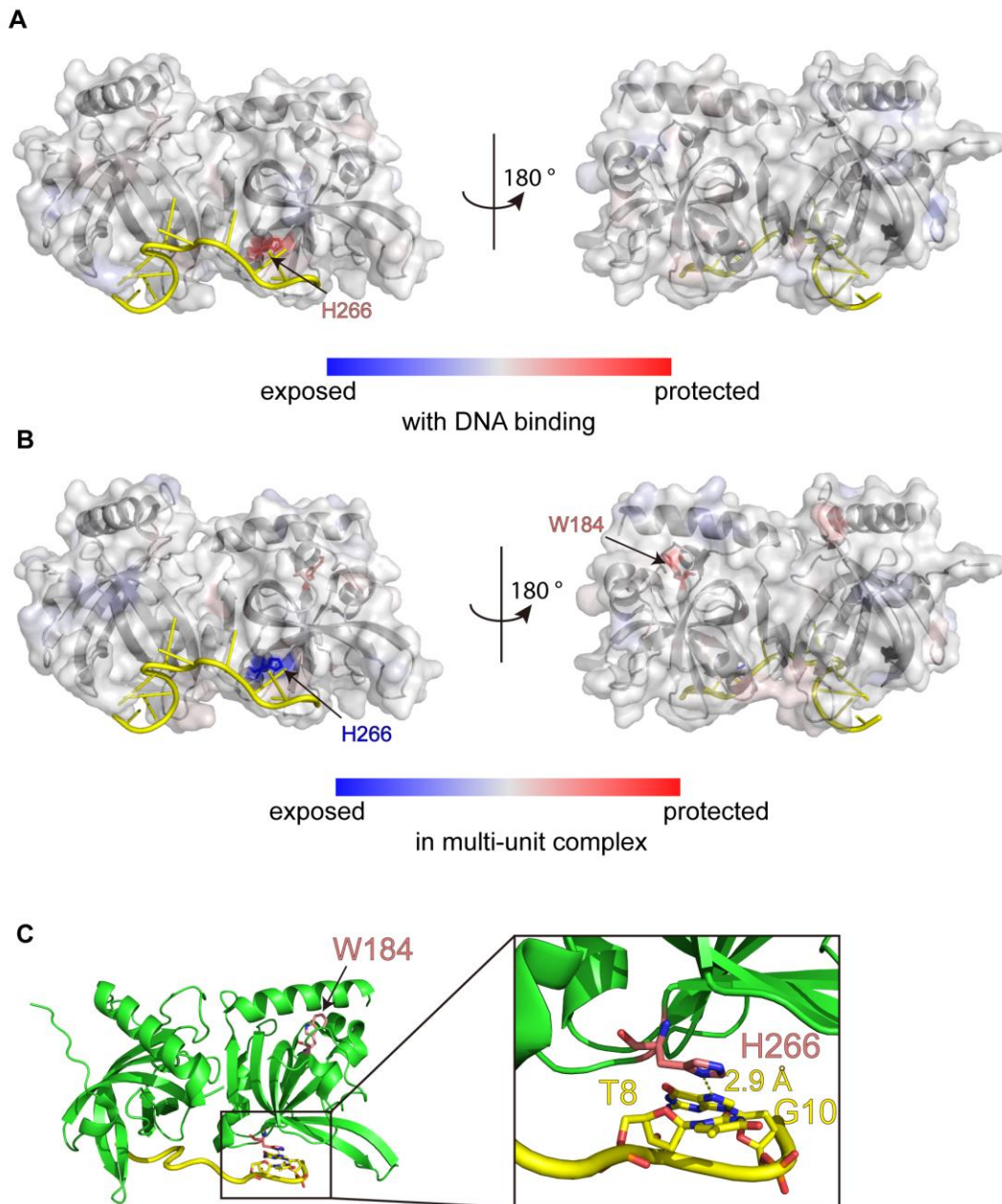


Figure S2. Regions of POT1-N that exhibit alterations in hydroxyl radical modification rates upon telomere ssDNA binding and oligomerization on long ssDNA. **A.** The structure of an individual POT1-N protein in complex with ssDNA (PDB ID: 1XJV) (1) was used for interpretation of HRF data. The structure is colored based on normalized modification rate ratios of POT1-N/POT1-N-hT12 (an individual protein with and without the minimal hT12 ssDNA substrate). Those residues identified with the most significant changes are highlighted in stick representations and labeled accordingly. The color bar indicates relative solvent accessibility. **B.** The data depicted are similar to that in panel **A** except that it is based on normalized modification rate ratios of POT1-N-hT12/POT1-N-hT72 (single protein on a short ssDNA substrate versus six proteins coating a long ssDNA substrate). The color bar indicates relative solvent accessibility. **C.** Structure of POT1-N (green) with hT10 (yellow). W184 and H266 residues highlighted in pink. Inset displays interactions between POT1 H266 and T8 and G10 of hT10 ssDNA. Hydrogen bond between H266 and G10 is indicated by dashed line.

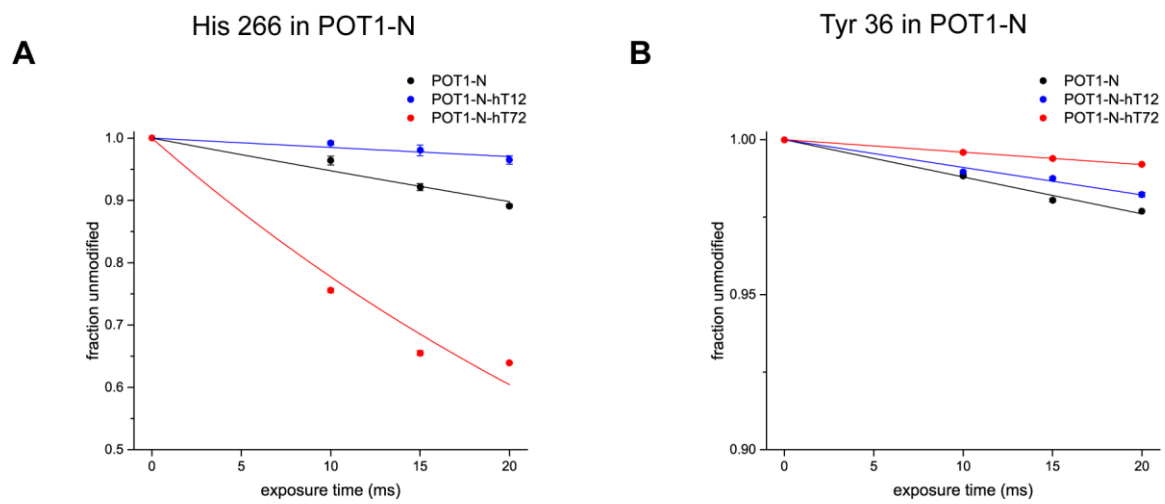


Figure S3. Oxidation rates of identified residues in POT1-N. Dose response curves for hydroxyl radical footprinting of **A.** H266 and **B.** Y36 of POT1-N for different DNA bound states (black for protein only, blue for protein bound to hT12 and red for protein bound to hT72).

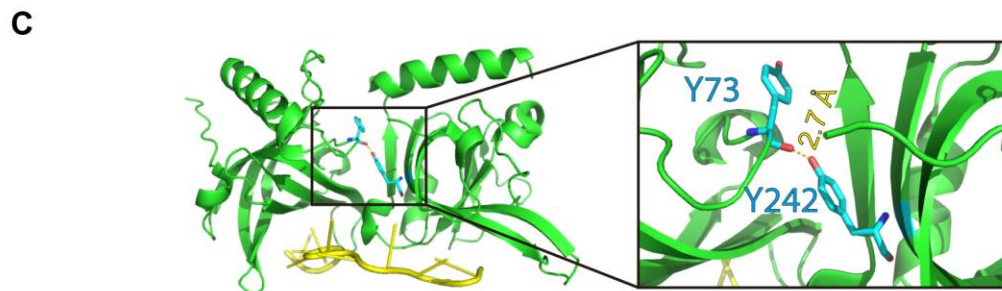
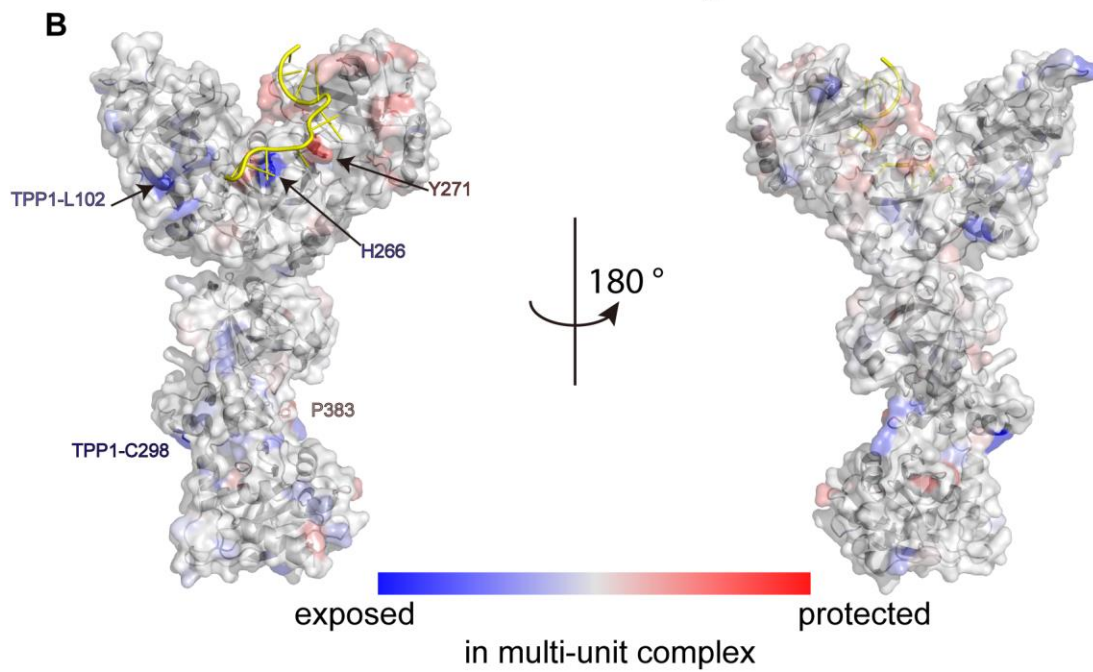
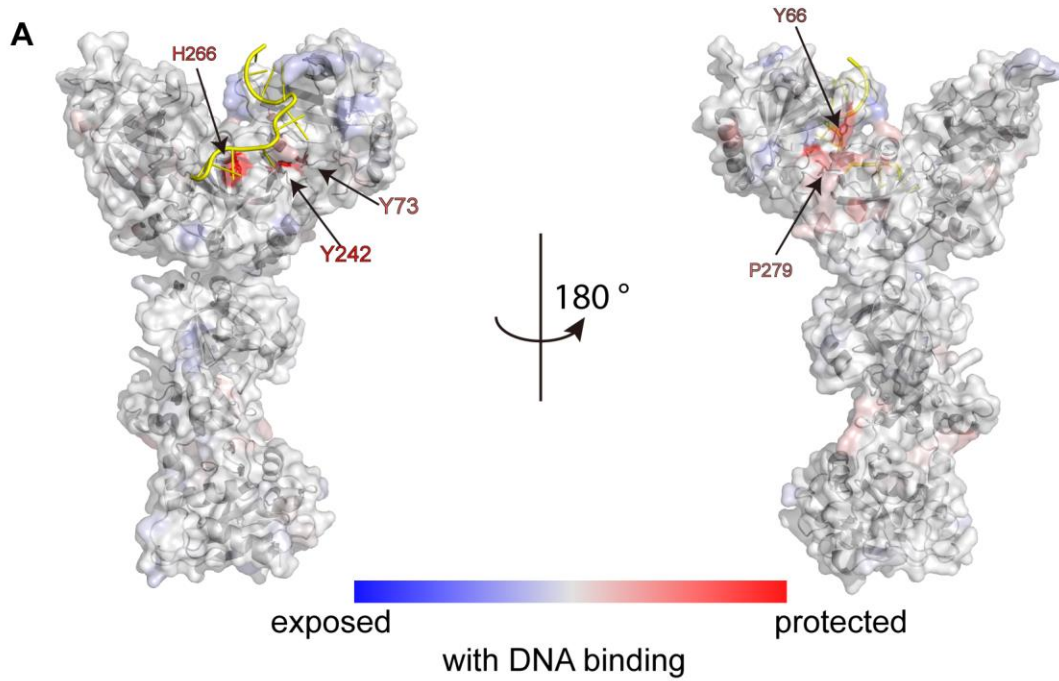


Figure S4. HRF results of POT1-TPP1 complexes bound to different telomere ssDNA substrates. A. Model of POT1-TPP1 complex with hT10 was assembled using POT1-N-hT10 (PDB ID: 1XJV) (1), TPP1 OB-fold (PDB ID: 2I46) (11) and POT1-C and TPP1 POT1-binding domain (PDB ID: 5UN7) (12) based on the organization of the telomere end-binding complex from *Oxytricha nova*, TEBP α -TEBP β -ssDNA (PDB ID: 1OTC) (13). Model is color coded to depict normalized modification rate ratios of PT/PT-hT12 (an individual protein complex with and without the minimal ssDNA substrate). Those residues identified with the most significant changes are highlighted in stick representations and labeled accordingly. **B.** The data depicted are similar to that in panel **A** except that it is based on normalized modification rate ratios of PT-hT12/PT-hT72 (single protein complex on a short ssDNA substrate versus six protein complexes coating a long ssDNA substrate). Color bars indicate relative normalized modification rate ratios. **C.** Structure of POT1-N with hT10. Y73 and Y242 residues highlighted in cyan. Inset displays hydrogen bond between the backbone carbonyl group of the Y73 and Y242 side chain hydroxyl group.

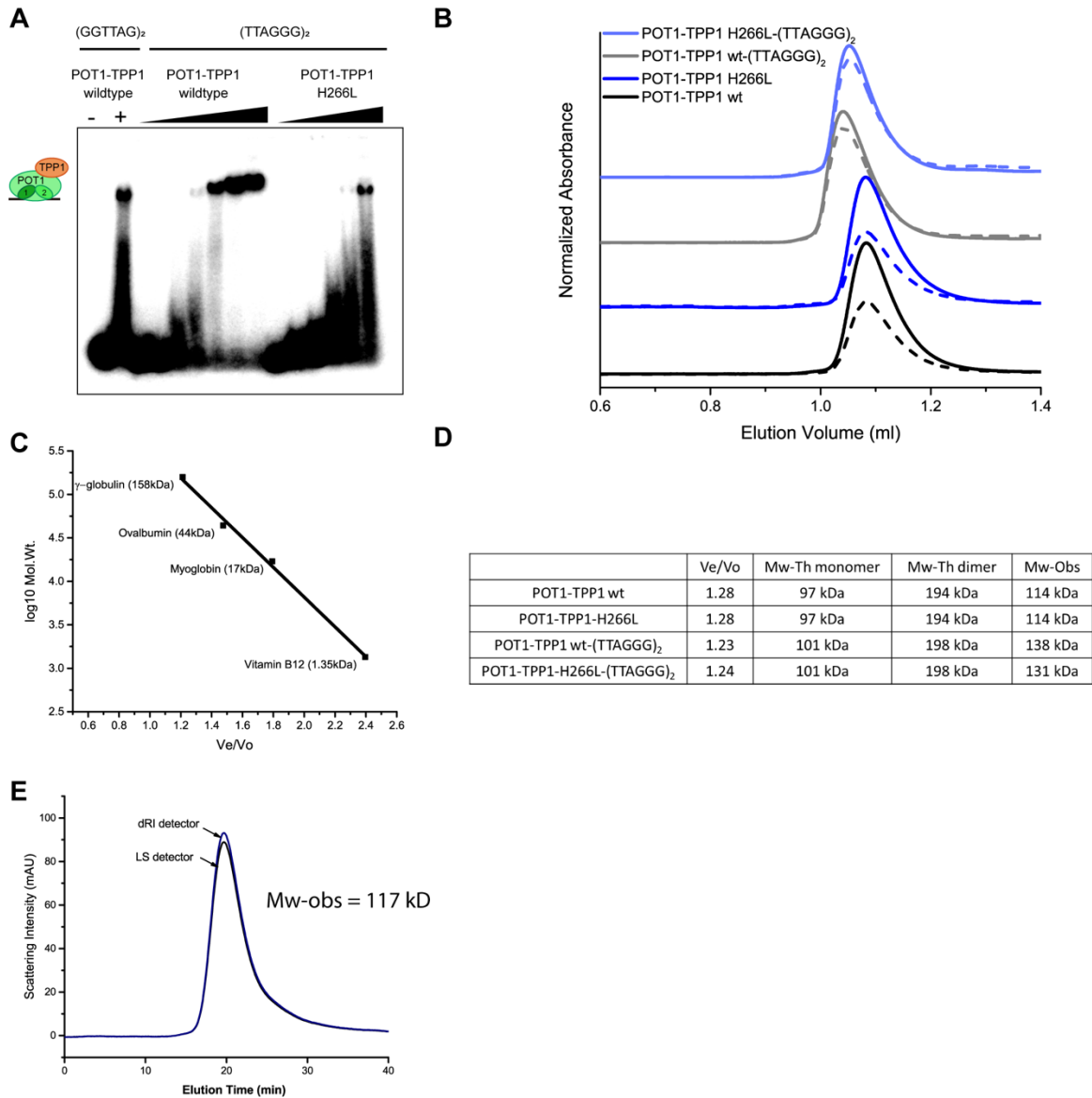


Figure S5. Wild type and H266L POT1-TPP1 protein exhibit one binding event on hT12 substrates. **A.** EMSA assays were performed under equilibrium binding conditions to identify the number of POT1-TPP1 proteins that bind to (GGTTAG)₂ and (TTAGGG)₂ telomeric substrates. Binding to (GGTTAG)₂ was performed with 0 (lane 1) or 10 nM (lane 2) POT1-TPP1 protein. Binding to the (TTAGGG)₂ substrate was performed using wild type POT1-TPP1 protein with concentrations ranging from 0 to 1 μ M (lanes 3-8), while H266L mutant POT1-TPP1 reaction concentrations ranged from 0 to 10 μ M (lanes 9-14). **B.** Size-exclusion chromatography of POT1-TPP1 with or without telomere ssDNA substrates (TTAGGG)₂. Profiles of the wild type POT1-TPP1, H266L mutant POT1-TPP1, wild type POT1-TPP1-(TTAGGG)₂, and H266L mutant POT1-TPP1-(TTAGGG)₂ are shown in black, blue, grey, and light blue, respectively, and as labeled. Absorbance at 280nm is shown as solid lines and the absorbance at 260nm is shown as dashed lines. **C.** Calibration of the size-exclusion column using protein standards. Ve=elution volume, Vo=void volume. **D.** Summary of size-exclusion analyses of wild-type and H266L POT1-TPP1 complexes. Mw-Th monomer and Mw-Th dimer are the theoretical molecular weights of complexes containing one and two POT1-TPP1 proteins. Mw-Obs is the molecular weight calculated based on Ve/Vo against that of molecular weight standards. **E.** Multi-angle light scattering (MALS) analysis of POT1-TPP1-hT12. Complex status was determined using Wyatt TREOS multi-angle light scattering. The resultant molecular weight (Mw-obs) for ssDNA-bound complex is displayed. dRI = differential refractive index, LS = light scattering.

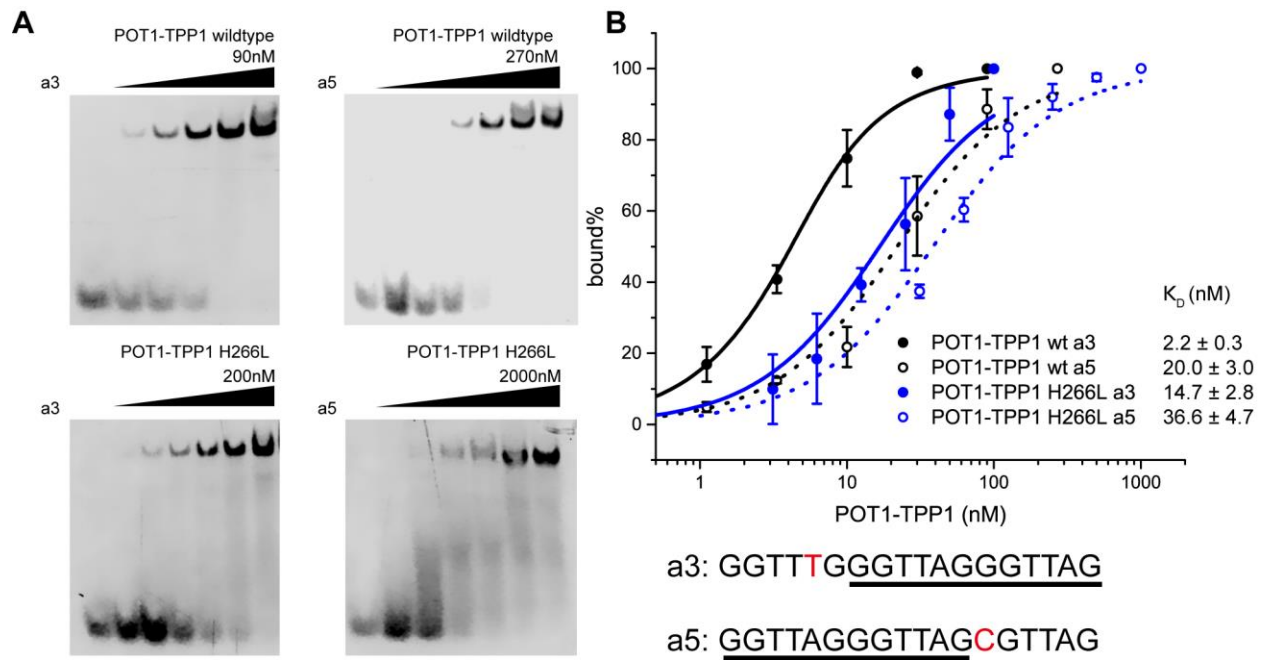


Figure S6. H266L mutation impairs the end-binding preference of POT1-TPP1. **A.** EMSA assays were performed to determine the effects of H266L mutant binding to a 3' (a3) or 5' (a5) recognition sequence in an 18-nt telomere ssDNA substrate. To obtain a reliable fitting curve, variable protein concentration ranges were used for different constructs and for different substrates, as indicated by highest protein concentration labeled for each gel shift. **B.** Quantification of EMSA data for POT1-TPP1 and H266L mutant protein binding to a3 and a5 primer. Dissociation constants (K_D) are indicated. Error bars represent the mean \pm SD ($n=3$). Sequence of primer a3 and a5 are shown below. The sequence underlined indicates the native POT1 recognition sequence. Point mutations to the telomere ssDNA sequence are highlighted in red.

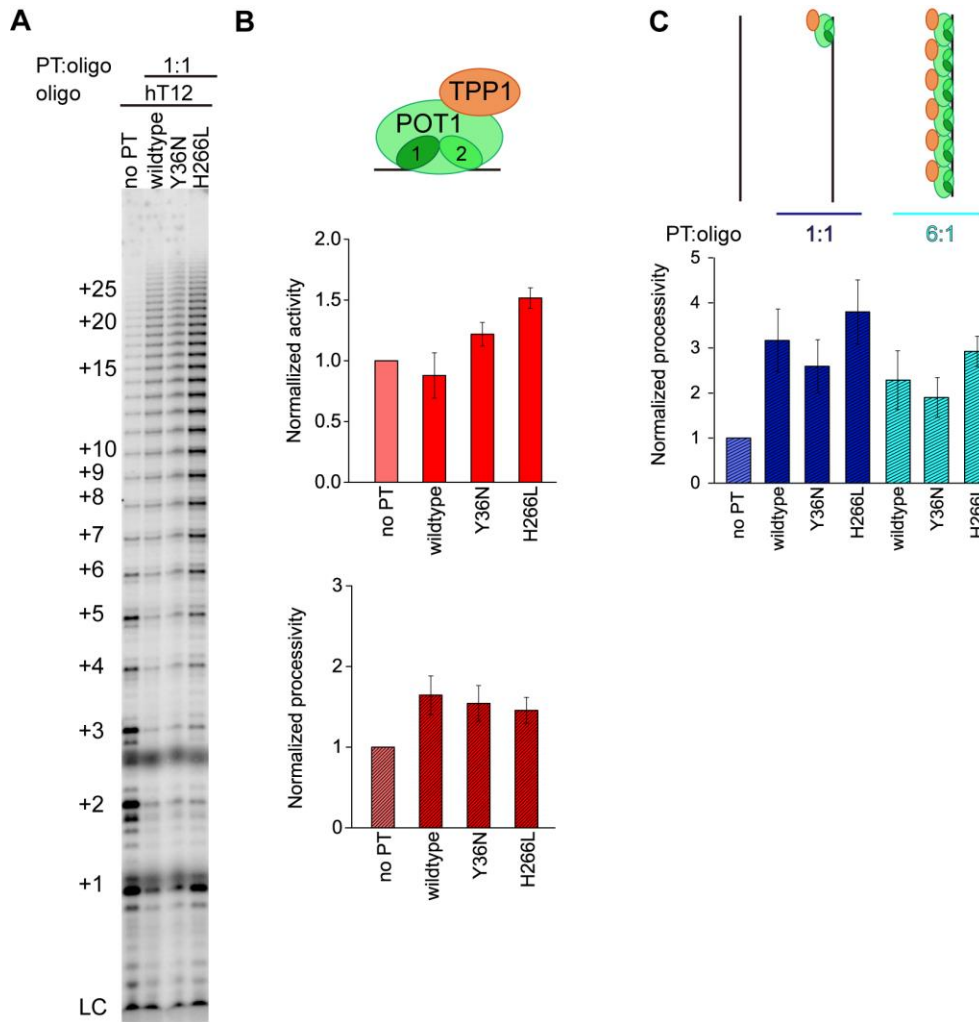


Figure S7. POT1-TPP1 wild type and mutant complexes enhance telomerase processivity to extend telomere ssDNA substrates. **A.** Direct *in vitro* telomerase assay performed on hT12 ssDNA. Lane 1: no POT1-TPP1 added. Lane 2-4: stoichiometric concentration of POT1-TPP1 wildtype, Y36N and H266L added, respectively. LC=Loading control. **B.** Quantification of lanes in panel **A** displaying normalized telomerase activity (upper panel) and processivity (lower panel). **C.** Quantification of data presented in **Figure 3A** displaying normalized telomerase processivity. Schematic models indicate the different binding states of POT1-TPP1 complexes binding to telomere ssDNA. Error bars represent the mean \pm SD (n=3).

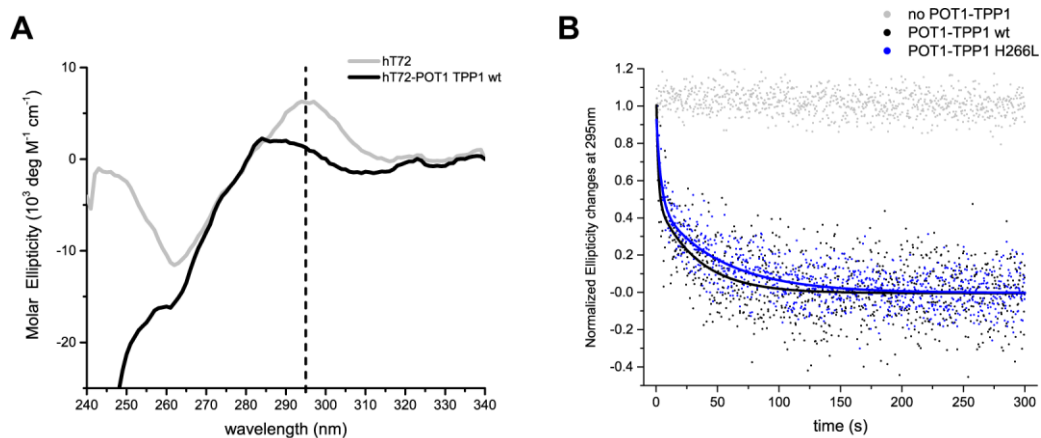
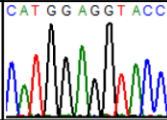
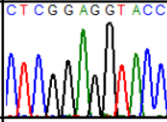
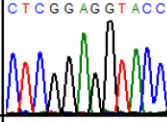
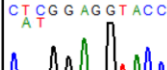
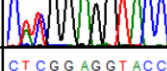
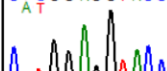



Figure S8. Destabilization of hT72 formed G-quadruplex upon POT1-TPP1 binding. **A.** CD spectra of hT72 before (grey line) and 300 seconds after mixing with POT1-TPP1 wild type (black line) protein. The dashed line indicates 295 nm that was recorded over time. **B.** Time-course for the circular dichroism signal at 295 nm of hT72 without (grey dots) and with mixing POT1-TPP1 wild type (black) or H266L mutant (blue) protein. Solid lines indicate double-exponential fits of the protein mixing data.

A

CAT->CTC H266L

cell lines	sequence	NGS total reading #	NGS mutated reading# (%)	Sanger Sequencing
parental	CATGGAGGTACC	NA	NA	
Homo #1	CTCGGAGGTACC	4037	3821 (94.6%)	
Homo #2	CTCGGAGGTACC	6422	6124 (95.4%)	
Het #1	WT:CATGGAGGTACC	7766	3621 (46.6%)	
	MUT:CTCGGAGGTACC			
Het #2	WT:CATGGAGGTACC	5715	2684 (47.0%)	
	MUT:CTCGGAGGTACC			

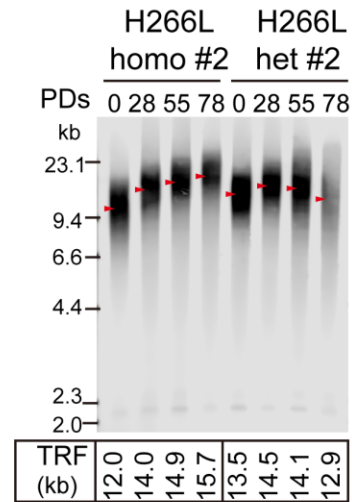
B

Figure S9. H266L POT1 mutant promotes telomere extension in cancer cell line. **A.** Validation of H266L substitution in HCT 116 cells. Cell lines edited by CRISPR-Cas9 and used for telomere restriction fragment (TRF) analysis were validated by NGS and Sanger sequencing to confirm the introduction of H266L substitution. **B.** TRF analysis of genomic DNA from CRISPR-Cas9 edited cell lines containing homozygous H266L (homo #2) and heterozygous H266L (het #2) POT1 mutations at the indicated population doublings (PDs) in culture. Quantified TRF lengths are indicated by red arrows and values shown below.

Table S1. Summary of hydroxyl radical modification rate constant for residues in POT1-N, POT1-N-hT12 and POT1-N-hT72.

Peptide	Sequence	Residues Modified	Modification Rate, S ⁻¹	Modification Rate, S ⁻¹	Modification Rate, S ⁻¹
			POT1-N	POT1-N-hT12	POT1-N-hT72
[-5-8]	GPLG S MSLVPATN	M1	80.6 ± 3.04	104.9 ± 4.8	76.4 ± 0.97
[-1-9]	S MSLVPATNY	M1	85.6 ± 5.04	109.6 ± 8.0	64.6 ± 2.2
[10-25]	I Y TPLN Q L K GGT I V N V	I10	0.97 ± 0.03	1.27 ± 0.05	1.1 ± 0.02
		L17	0.46 ± 0.02	0.71 ± 0.06	0.55 ± 0.012
		K18	1.33 ± 0.05	1.7 ± 0.06	1.4 ± 0.04
		I22	1.30 ± 0.13	2.4 ± 0.18	1.1 ± 0.03
[25-31]	VYGVV K F	no mod	-	-	-
[31-43]	FKPP Y L S K G T D Y	L37	0.47 ± 0.04	0.71 ± 0.02	0.29 ± 0.01
		K39	1.20 ± 0.03	1.55 ± 0.06	0.61 ± 0.03
		Y43	1.25 ± 0.04	1.43 ± 0.03	0.50 ± 0.015
[31-42]	FKPP Y L S K G T D	Y36	1.2 ± 0.027	0.90 ± 0.029	0.40 ± 0.008
		L37	0.58 ± 0.02	0.84 ± 0.029	0.33 ± 0.013
		K39	0.62 ± 0.032	0.67 ± 0.038	0.29 ± 0.005
[49-57]	I V D Q T N V K L	I49orV50	0.21 ± 0.013	0.22 ± 0.013	0.20 ± 0.005
		V55	0.49 ± 0.028	0.51 ± 0.015	0.50 ± 0.011
		K56	0.75 ± 0.015	0.81 ± 0.0157	0.86 ± 0.017
[60-66]	LLFSG N Y	no mod	-	-	-
[62-69]	FSG N Y E A L	no mod	-	-	-
[70-77]	P I Y K NGD	I71	0.27 ± 0.005	0.29 ± 0.010	0.14 ± 0.002
		Y73	0.63 ± 0.023	0.81 ± 0.017	0.54 ± 0.019
[70-81]	P I Y K NGD I V R F	I71	0.22 ± 0.012	0.27 ± 0.005	0.14 ± 0.003
		Y73	0.67 ± 0.021	0.86 ± 0.023	0.54 ± 0.009
[82-101]	HRL K I Q V Y K ET Q G I T S S G F	K90	8.32 ± 0.34	11.88 ± 0.57	9.33 ± 0.34
		I96	6.16 ± 0.21	7.49 ± 0.55	8.50 ± 0.29
[89-101]	Y K ET Q G I T S S G F	K90	2.58 ± 0.025	5.7 ± 0.12	2.56 ± 0.048
[105-122]	TFEG T L G A P I P R T S S K Y	L110	0.82 ± 0.074	1.0 ± 0.09	1.03 ± 0.022
		I115	2.5 ± 0.08	3.1 ± 0.17	0.8 ± 0.043
		K121	1.6 ± 0.075	2.5 ± 0.11	2.8 ± 0.11
[113-125]	P I P R T S S K Y F N F	I115	2.25 ± 0.08	3.25 ± 0.26	0.58 ± 0.018
		K121	1.76 ± 0.063	2.1 ± 0.061	1.6 ± 0.0423
		Y122	2.5 ± 0.082	3.6 ± 0.082	3.0 ± 0.13
		F125	0.69 ± 0.03	1.1 ± 0.078	0.63 ± 0.047
[123-135]	FN F T E D H K M V E A	M132	32.84 ± 1.35	43.34 ± 2.42	35.25 ± 1.89
[139-148]	W A S T H M S P S W	M144	25.43 ± 1.07	25.74 ± 1.03	12.14 ± 0.72
[139-150]	W A S T H M S P S W T L	M144	25.65 ± 1.02	26.34 ± 1.16	13.40 ± 0.74
[151-161]	L K L C D V Q P M Q Y	M159	36.83 ± 1.20	56.26 ± 3.71	37.05 ± 2.06
[162-168]	F D L T C Q L	No mod	-	-	-
[169-179]	L G K A E V D G A S F	K171	0.35 ± 0.034	0.33 ± 0.019	0.17 ± 0.006
		E173	0.48 ± 0.046	0.40 ± 0.035	0.23 ± 0.017
[169-180]	L G K A E V D G A S F L	K171	0.32 ± 0.022	0.31 ± 0.014	0.16 ± 0.004
		E173	0.46 ± 0.010	0.45 ± 0.016	0.23 ± 0.005
[181-194]	L K V W D G T R T P F P S W	R188	0.26 ± 0.010	0.24 ± 0.027	0.17 ± 0.027
		F191	3.66 ± 0.16	4.83 ± 0.18	1.94 ± 0.017
		W194/W184	7.48 ± 0.12	6.02 ± 0.46	0.43 ± 0.007
		W194	0.46 ± 0.036	0.48 ± 0.032	0.38 ± 0.039
[195-200]	R V L I Q D	No mod	-	-	-
[204-216]	E G D L S H I H R L Q N L	L207	0.61 ± 0.028	0.61 ± 0.025	0.56 ± 0.013
		H209	0.49 ± 0.029	0.77 ± 0.059	0.39 ± 0.020
		H211	2.14 ± 0.049	3.01 ± 0.095	1.40 ± 0.018
[222-232]	V Y D N H V H V A R S	Y223	1.48 ± 0.039	1.29 ± 0.078	0.48 ± 0.016
		H228	4.27 ± 0.14	4.46 ± 0.17	2.06 ± 0.12

Peptide	Sequence	Residues Modified	Modification Rate, S ⁻¹	Modification Rate, S ⁻¹	Modification Rate, S ⁻¹
			POT1-N	POT1-N-hT12	POT1-N-hT72
[222-238]	VYDNHVVHVARSLKVGSF	Y223	0.91 ± 0.031	0.90 ± 0.046	0.31 ± 0.019
		H228	2.34 ± 0.14	3.01 ± 0.094	0.76 ± 0.089
		K234	1.38 ± 0.035	1.45 ± 0.059	0.85 ± 0.023
		F239	0.69 ± 0.045	1.39 ± 0.099	0.53 ± 0.039
[239-244]	LRIYSL	Y242	0.51 ± 0.03	0.44 ± 0.022	0.12 ± 0.009
[245-258]	HTKLQSMNSENQTM	M251	42.35 ± 1.86	44.59 ± 1.68	36.71 ± 2.04
[263-274]	FHLHGGTSYGRG	H264	4.42 ± 0.33	5.59 ± 0.16	2.15 ± 0.13
[264-275]	HLHGGTSYGRG	H266	5.34 ± 0.31	1.50 ± 0.21	25.39 ± 1.10
[275-284]	IRVLPESNSD	No mod	-	-	-
[290-297]	VDQLKKDLESANL	K289/K290	1.26 ± 0.036	1.37 ± 0.042	1.34 ± 0.036
		L297	0.41 ± 0.019	0.53 ± 0.061	0.47 ± 0.012
[298-305]	TANQHSDV	No mod	-	-	-
[308-318]	QSEPDDSFNG	No mod	-	-	-
[319-327]	VSLRPPGWS	W326	11.00 ± 0.41	11.89 ± 0.34	11.76 ± 0.61

Table S2. Summary of hydroxyl radical modification ratios for residues in comparison of POT1-N/POT1-N-hT12 and POT1-N-hT12/POT1-N-hT72.

Residue number	Residue	Normalized modification ratio	Normalized modification ratio
		POT1-N /POT1-N-hT12	POT1-N-hT12 /POT1-N-hT72
1	M	0.92	0.89
10	I	0.91	0.67
17	L	0.77	0.75
18	K	0.93	0.71
22	I	0.65	1.27
36	Y	1.59	1.31
37	L	0.81	1.45
39	K	1.01	1.41
43	Y	1.04	1.66
49	I	1.14	0.64
50	V	1.14	0.64
55	V	1.15	0.59
56	K	1.11	0.55
71	I	1.04	1.16
73	Y	0.93	0.90
90	K	0.67	0.98
96	I	0.98	0.51
110	L	0.98	0.56
115	I	0.89	2.71
121	K	0.87	0.63
122	Y	0.83	0.70
125	F	0.75	1.01
132	M	0.90	0.71
144	M	1.17	1.19
159	M	0.78	0.88
171	K	1.25	1.13
173	E	1.32	1.07

Residue number	Residue	Normalized modification ratio	Normalized modification ratio
		POT1-N /POT1-N-hT12	POT1-N-hT12 /POT1-N-hT72
184	W	1.48	8.14
188	R	1.29	0.82
191	F	0.90	1.45
194	W	1.30	2.44
207	L	1.19	0.63
209	H	0.76	1.15
211	H	0.85	1.25
223	Y	1.29	1.62
228	H	1.03	1.70
234	K	1.14	0.99
239	L	0.59	1.52
242	Y	1.38	2.13
251	M	1.13	0.71
264	H	0.94	1.51
266	H	4.25	0.03
289	K	1.10	0.59
290	K	1.10	0.59
297	L	0.92	0.66
326	W	1.09	0.63
*normalization factor		0.84	1.72
† mean-3SD		0.42	0.11
† mean-2SD		0.56	0.22
† mean		1.03	0.95
† mean+2SD		1.89	4.04
† mean+3SD		2.56	8.36

*The normalization factor is determined as the average of mean and median from all identified ratios of modification rates before normalization in log₁₀ scale, then converted back to linear scale.

† mean and SD are also calculated based on normalized modification rate ratios in log₁₀ scale, then mean±2SD and mean±3SD are determined, and finally converted back to linear scale.

Table S3. Summary of hydroxyl radical modification rate constant for residues in PT, PT-hT12, and PT-hT72.

Peptide	Sequence	Residues Modified	Modification Rate, s ⁻¹	Modification Rate, s ⁻¹	Modification Rate, s ⁻¹
			PT	PT-hT12	PT-hT72
POT1					
[1-9]	MSLV P ATNY	M1	1240.0 ± 216.7	1510.0 ± 108.4	565.86 ± 34.11
[2-9]	SLV P ATNY	L3	76.39 ± 3.67	78.29 ± 5.73	23.10 ± 1.85
		Y9	76.0 ± 5.10	73.71 ± 3.80	23.0 ± 1.13
[9-17]	Y I Y T PLNQL	Y9	174.34 ± 8.29	175.34 ± 13.24	48.04 ± 3.37
		I10	179.21 ± 5.50	215.76 ± 21.55	60.30 ± 4.16
[10-24]	IY T PLNQL K GGTIV N	K18	179.44 ± 9.39	214.58 ± 13.29	41.92 ± 2.49
[10-25]	I Y TPLNQL K GGTIV NV	I10	53.42 ± 4.64	60.59 ± 4.27	16.24 ± 1.04
		K18	164.83 ± 13.16	200.92 ± 16.13	38.99 ± 1.93
		I22	104.43 ± 6.60	144.52 ± 14.29	39.79 ± 3.29
[30-36]	VYGV V KF	no mod	-	-	-
[32-37]	FK P P Y L	Y36	51.25 ± 1.86	53.42 ± 2.96	8.46 ± 0.56
[32-43]	FK P P Y L S KGTDY	Y36	51.18 ± 2.72	62.38 ± 3.87	10.27 ± 0.64
		L37	19.63 ± 1.66	35.19 ± 2.65	7.90 ± 0.44
		K39	53.55 ± 2.07	80.46 ± 6.64	14.38 ± 1.57
[32-42]	FK P P Y L S KGTD	Y36	40.93 ± 2.45	41.57 ± 2.83	7.25 ± 0.49
		L37	25.78 ± 1.53	43.29 ± 2.54	8.51 ± 0.47
		K39	36.26 ± 1.95	54.96 ± 2.58	9.39 ± 0.67
[49-57]	I V DQ T N V K L	V55	322.96 ± 14.02	441.48 ± 23.22	74.75 ± 11.42
		K56	213.87 ± 5.99	282.08 ± 19.76	68.38 ± 7.95
[61-66]	L F S G N Y	Y66	137.23 ± 8.13	44.06 ± 2.85	9.21 ± 0.74
[70-77]	P I Y K NGD	I71	11.89 ± 0.55	15.57 ± 1.24	5.11 ± 0.25
		Y73	69.09 ± 1.95	13.83 ± 0.90	3.66 ± 0.50
[82-88]	H R L K I Q V	no mod	-	-	-
[89-100]	Y K K E T Q G I T S S G	Y89/K90/K91	155.92 ± 4.99	208.71 ± 17.72	44.45 ± 3.15
[89-101]	Y K K E T Q G I T S S G F	Y89/K90	153.45 ± 4.47	216.38 ± 18.85	52.84 ± 3.13
[105-112]	T F E G T L G A	no mod	-	-	-
[105-122]	T F E G T L G A P I P R T S S K Y	L110	1990.0 ± 159.4	1810.0 ± 194.2	491.33 ± 36.08
		P113	106.06 ± 6.17	119.55 ± 11.08	66.19 ± 4.56
		K121	84.31 ± 9.68	80.82 ± 4.57	61.43 ± 3.63
		Y122	89.08 ± 6.28	100.87 ± 11.1	34.26 ± 4.99
[113-122]	P I P R T S S K Y	I115	14.89 ± 0.87	20.08 ± 1.42	7.46 ± 0.53
		Y122	61.60 ± 3.45	64.19 ± 3.82	19.60 ± 0.74
[125-135]	F T T E D H K M V E A	M132	218.10 ± 12.51	286.79 ± 18.96	155.39 ± 2.10
[126-135]	T T E D H K M V E A	H130	33.31 ± 1.97	21.56 ± 1.68	6.47 ± 0.32
		M132	34.30 ± 2.62	44.20 ± 1.46	33.44 ± 4.44
[139-150]	W A S T H M S P S W T L	M144	627.06 ± 27.10	552.03 ± 42.68	85.27 ± 5.55
[143-150]	H M S P S W T L	H143	39.07 ± 1.44	41.01 ± 2.90	14.41 ± 1.02
		M144	128.32 ± 6.61	101.88 ± 5.96	29.21 ± 2.34
[151-160]	L K L C D V Q P M Q	M159	1840.0 ± 106.9	2180.0 ± 164.1	706.62 ± 46.6
[152-161]	K L C D V Q P M Q Y	C154	713.72 ± 62.79	528.61 ± 55.62	173.46 ± 13.97
		M159	510.78 ± 15.48	728.65 ± 67.89	182.36 ± 10.94
[162-168]	F D L T C Q L	No mod	-	-	-
[169-179]	L G K A E V D G A S F L	L169	4.26 ± 0.14	2.37 ± 0.15	1.33 ± 0.21
		K171	17.46 ± 0.76	13.57 ± 1.08	5.14 ± 0.32
		E173	29.32 ± 0.49	26.42 ± 1.98	6.31 ± 0.45
		V174	8.21 ± 0.26	8.54 ± 0.76	1.47 ± 0.063
		A177	22.86 ± 0.60	26.56 ± 2.12	5.97 ± 0.28
[180-194]	L L K V W D G T R T P F P S W	W184	43.56 ± 3.53	53.41 ± 3.70	17.36 ± 1.38
		P190	34.03 ± 2.0	32.22 ± 2.48	25.89 ± 2.09
		F191	66.24 ± 4.89	105.55 ± 7.46	22.17 ± 1.65

Peptide	Sequence	Residues Modified	Modification Rate, s ⁻¹	Modification Rate, s ⁻¹	Modification Rate, s ⁻¹
			PT	PT-hT12	PT-hT72
		W194	7.78 ± 0.35	7.16 ± 0.31	1.30 ± 0.083
		W184/W194	28.9 ± 0.89	27.93 ± 2.69	11.49 ± 0.79
[181-194]	LKV W DG T R T P F P S W	W184	36.57 ± 3.45	47.07 ± 2.63	16.39 ± 1.23
		P190	29.83 ± 2.21	39.19 ± 3.15	20.71 ± 1.36
		F191	54.29 ± 0.32	93.77 ± 9.02	18.51 ± 1.49
		W194	6.86 ± 0.32	5.42 ± 0.16	1.05 ± 0.084
		W184/W194	23.82 ± 2.47	26.85 ± 1.59	8.43 ± 0.69
[195-200]	RV L I Q D	L197	87.80 ± 4.91	83.95 ± 6.74	16.66 ± 0.61
[204-216]	EGDLSH I HRLQNL	H211	154.95 ± 12.75	161.81 ± 11.86	40.65 ± 1.21
[208-216]	SH I HRLQNL	H209	838.6 ± 38.1	886.7 ± 55.1	374.0 ± 26.8
[220-232]	ILVYDNH V HVAR S	No mod	-	-	-
[222-232]	V Y DNH V HVAR S L KV G S	Y223	66.39 ± 1.94	74.30 ± 4.85	12.67 ± 0.77
		H228	284.85 ± 27.02	195.67 ± 11.27	37.43 ± 2.28
[223-232]	YDNH V HVAR S LK V G S	H228	295.78 ± 21.45	190.29 ± 16.85	46.14 ± 3.34
[230-238]	AR S L K V G S F	L233	77.08 ± 5.37	42.87 ± 2.68	11.39 ± 1.54
		K234	148.04 ± 6.58	125.88 ± 12.63	25.28 ± 3.16
[239-244]	L R I Y S L	I241	9.82 ± 0.64	11.59 ± 0.62	3.18 ± 0.23
		Y242	114.04 ± 3.45	11.4 ± 0.69	5.58 ± 0.62
[245-256]	HTKL Q S M NS E N Q	M251	645.13 ± 22.28	887.53 ± 69.15	253.41 ± 5.06
[264-274]	HL H GG T S Y GR G	H266	232.16 ± 11.43	34.01 ± 2.11	59.55 ± 4.26
		Y271	48.96 ± 1.07	32.38 ± 1.07	3.92 ± 0.31
[275-284]	IR V L P ES N SD	V277	53.24 ± 1.75	26.31 ± 1.55	8.70 ± 0.25
		P279	48.24 ± 1.55	19.23 ± 1.16	6.43 ± 0.83
		E280	41.82 ± 1.39	29.82 ± 2.08	7.48 ± 0.64
[275-287]	IR V L P ES N SD V D Q	V277	51.16 ± 2.57	27.33 ± 1.39	10.60 ± 0.57
		P279	89.58 ± 6.13	36.28 ± 2.31	10.00 ± 0.14
		E280	101.87 ± 5.07	74.98 ± 5.82	17.69 ± 1.29
[285-297]	VD Q L K KD L ES A N L	K289/K290	219.79 ± 4.29	169.06 ± 10.24	54.71 ± 2.63
		L297	40.63 ± 3.33	41.59 ± 1.21	15.25 ± 1.43
[298-307]	TAN Q HSD V I C	No mod	-	-	-
[306-323]	IC Q SE P DD S FP S SG SV S L	No mod	-	-	-
[324-329]	YE V ER C	No mod	-	-	-
[335-343]	T I L T D H Q Y L	D339	27.26 ± 1.46	26.40 ± 2.22	9.13 ± 0.65
		Y342	23.78 ± 1.60	28.36 ± 2.38	8.07 ± 0.34
[342-350]	Y L E R T P L C A	Y342	53.52 ± 4.11	46.01 ± 3.31	14.83 ± 0.21
[351-359]	IL K Q K A P Q Q	Q354/K355	80.37 ± 2.57	79.58 ± 5.73	26.98 ± 1.74
[360-366]	Y R I R A K L	Y360	35.50 ± 1.05	37.99 ± 2.0	7.49 ± 0.51
[367-376]	R S Y K P R R L F Q	Y369/K370	95.29 ± 2.14	82.30 ± 4.67	21.61 ± 1.07
[377-387]	SV K L H C P K C H L	P383	22.17 ± 0.16	22.68 ± 0.22	2.52 ± 0.21
		K384	10.68 ± 0.51	7.46 ± 0.61	6.33 ± 0.49
		H386	14.87 ± 1.31	10.69 ± 1.04	8.61 ± 0.57
[388-397]	L Q E V P H E G D L	P392	28.22 ± 2.78	23.04 ± 2.23	12.5 ± 0.83
		H393	26.73 ± 1.60	22.51 ± 1.35	6.40 ± 0.48
[399-405]	I I F Q D G A	No mod	-	-	-
[419-438]	Y D S K I W T T K N Q K GR K V A V H F	K422	177.96 ± 9.90	226.15 ± 7.39	201.93 ± 11.22
		K427	169.89 ± 9.19	216.39 ± 12.23	96.56 ± 4.55
[439-449]	V K N N G I L P L S N	I444	35.59 ± 1.32	30.63 ± 2.32	18.50 ± 1.04
		L445/L447	84.62 ± 3.79	73.50 ± 4.85	38.40 ± 2.16
[439-450]	V K N N G I L P L S N E	I444	59.29 ± 2.31	55.23 ± 3.48	29.07 ± 1.74
		L445/L447	106.63 ± 3.55	96.81 ± 5.92	52.51 ± 3.23
		P449	13.33 ± 0.90	13.76 ± 0.98	7.27 ± 0.47
[461-470]	SE I C K L S N K F	C464	2670.0 ± 303.9	2360.0 ± 185.8	532.32 ± 31.48

Peptide	Sequence	Residues Modified	Modification Rate, s ⁻¹	Modification Rate, s ⁻¹	Modification Rate, s ⁻¹
			PT	PT-hT12	PT-hT72
[471-481]	NSVIPVRS GHE	H480	487.73 ± 25.99	491.64 ± 37.01	156.32 ± 8.58
[471-485]	NSVIPVRS GHE DL EL	H480	72.93 ± 4.63	75.86 ± 4.65	25.18 ± 1.84
		E481	35.77 ± 2.10	37.39 ± 2.67	22.80 ± 1.42
[486-493]	LDLS A PFL	L488	543.47 ± 44.40	490.03 ± 47.35	84.56 ± 12.66
		S489	213.62 ± 19.95	193.08 ± 23.05	29.37 ± 2.73
[494-509]	IQGT IHHY GCKQC SSL	I498	49.28 ± 3.15	40.90 ± 3.39	30.98 ± 1.34
		H499/H500	18.02 ± 1.92	14.68 ± 1.17	5.18 ± 0.23
		Y501	64.75 ± 3.58	48.32 ± 4.58	25.91 ± 1.94
[516-528]	NSL V DKTSWIPSS	V519	2180.0 ± 205.3	2650.0 ± 228.9	470.13 ± 20.67
[516-530]	NSL V DKTSWIPSS VA	L518	196.44 ± 22.56	187.77 ± 17.0	54.87 ± 3.33
		V519	1830.0 ± 208.0	2080.0 ± 239.58	431.08 ± 27.37
[531-539]	EAL G IVPLQ	L533	145.49 ± 9.77	162.53 ± 12.92	35.25 ± 1.51
[533-539]	L G IVPLQ	V536	34.67 ± 1.15	29.16 ± 1.71	12.32 ± 0.38
[546-555]	FTLDD G T G VL	T552	7.67 ± 0.43	8.79 ± 0.62	2.88 ± 0.19
		V554	30.73 ± 0.69	30.56 ± 2.26	9.90 ± 0.73
[558-565]	Y L MDS D KF	Y558	126.35 ± 11.52	139.91 ± 14.25	67.91 ± 5.76
		M560	204.26 ± 11.89	231.44 ± 14.00	66.33 ± 5.21
[566-572]	F Q I P A S E	Q567	10.09 ± 0.30	9.90 ± 0.69	3.02 ± 0.21
		I568	9.32 ± 0.30	6.95 ± 0.57	3.56 ± 0.27
		P569	32.33 ± 1.26	29.29 ± 1.89	10.75 ± 0.77
[573-579]	V L MDDDL	M575	1320.0 ± 48.37	1440.0 ± 91.68	806.17 ± 43.48
[585-589]	M IMDM	M585	1120.0 ± 73.47	1320.0 ± 88.49	693.45 ± 81.89
[589-599]	M FCPPG I KIDA	M589	414.79 ± 24.75	518.58 ± 47.82	272.45 ± 9.27
[590-599]	F C PP G I K IDA	P593	27.91 ± 1.04	27.22 ± 2.68	8.30 ± 0.71
		K596	33.51 ± 2.06	34.86 ± 3.11	13.20 ± 0.86
[607-619]	IKSY N V T NGTD N Q	Y610	19.86 ± 0.57	17.05 ± 0.89	8.73 ± 0.35
		Q619	29.57 ± 1.05	24.79 ± 1.23	11.33 ± 0.47
[607-621]	IKSY N V T NGTD N Q I C	C621	250.81 ± 11.98	197.20 ± 12.60	92.76 ± 6.79
[623-628]	Q I F DTT	F625	90.66 ± 3.79	69.55 ± 6.26	52.77 ± 4.70
TPPI					
[94-101]	V L R P WIRE	L95	42.87 ± 3.80	38.52 ± 1.93	20.62 ± 1.09
		P97	90.33 ± 2.92	66.44 ± 3.44	58.84 ± 3.45
		W98	43.88 ± 3.73	48.60 ± 2.88	27.08 ± 2.58
[96-101]	R P WIRE	P97	67.96 ± 3.04	65.68 ± 5.50	54.93 ± 2.88
		W98	43.90 ± 1.18	41.65 ± 3.04	22.76 ± 1.42
[102-117]	L I L G SET P SS P RAG QL	L102	19.46 ± 1.61	19.83 ± 1.07	24.74 ± 2.94
		L104	76.87 ± 6.18	75.48 ± 3.44	62.33 ± 7.14
		P109	135.22 ± 8.02	128.90 ± 9.69	106.48 ± 5.25
[205-117]	G S ET P SS P RAG Q L	P109	142.54 ± 5.32	114.94 ± 8.16	93.42 ± 2.92
[127-141]	AVAG P SHAP D TSD VG	P131	96.28 ± 6.78	118.59 ± 12.13	107.39 ± 7.45
		H133	44.02 ± 4.62	52.46 ± 4.45	25.65 ± 1.78
[145-155]	L V SD G T H SVRC	V146	28.94 ± 1.97	23.90 ± 1.79	15.77 ± 0.92
		H151	32.14 ± 2.36	27.91 ± 2.09	9.98 ± 0.45
[172-181]	F GFR G TE G R L	F172	104.92 ± 5.81	89.90 ± 5.56	72.11 ± 3.32
[182-192]	LL Q DC G V H V Q	No mod	-	-	-
[202-206]	F YL Q V	F202/Y203	157.92 ± 8.20	114.05 ± 9.38	67.06 ± 5.94
[203-209]	Y L Q V DR F	Y203	31.85 ± 1.94	26.89 ± 0.74	15.46 ± 0.51
		D207	11.90 ± 1.03	9.03 ± 0.50	4.69 ± 0.40
		R208	72.29 ± 3.75	53.47 ± 4.51	29.62 ± 1.39
[213-228]	PTE Q PRL R V P G C N Q D L	C224	284.60 ± 15.94	314.16 ± 19.57	171.21 ± 8.71

Peptide	Sequence	Residues Modified	Modification Rate, s ⁻¹	Modification Rate, s ⁻¹	Modification Rate, s ⁻¹
			PT	PT-hT12	PT-hT72
[229-238]	DVQKKLYDCL	Y235	78.0 ± 5.59	72.97 ± 4.91	65.26 ± 3.67
		C237	77.63 ± 5.85	65.19 ± 6.33	27.28 ± 2.05
[239-254]	EEHLESTSSNAGLSL	No mod	-	-	-
[261-271]	MREDQEHQ GAL	M261	331.3 ± 19.17	621.11 ± 40.87	238.09 ± 11.64
		H267	35.76 ± 3.14	39.23 ± 1.53	7.83 ± 0.43
[280-293]	TLEGPCTAPPVTHW	L281	17.33 ± 1.34	17.38 ± 1.15	8.90 ± 0.74
		P284	54.67 ± 2.64	65.45 ± 5.09	27.94 ± 2.63
		C285	35.97 ± 2.50	38.80 ± 3.07	12.07 ± 1.27
		P288	23.76 ± 2.16	27.77 ± 2.08	18.39 ± 1.39
		H292	11.14 ± 0.81	11.70 ± 0.85	5.73 ± 0.57
[294-305]	AASRCKATGEAV	C298	1000.0 ± 46.59	650.46 ± 56.19	2300.0 ± 166.26
[306-312]	YTVPSSM	M312	117.07 ± 7.98	151.85 ± 6.21	60.27 ± 2.47
[306-313]	YTVPSSML	M312	1840.0 ± 55.04	2160.0 ± 162.0	1030.0 ± 57.59
[318-323]	NDQLIL	L321	290.62 ± 16.88	297.90 ± 16.76	111.32 ± 5.71
		I322	263.50 ± 9.79	287.61 ± 20.89	111.87 ± 4.47
[324-334]	SSLGPCQRTQG	P328	15.13 ± 0.59	15.40 ± 0.44	5.33 ± 0.16
		C329	35.28 ± 2.50	39.31 ± 2.67	21.69 ± 1.34
		R331	44.98 ± 3.05	43.39 ± 3.56	21.80 ± 1.88

Table S4. Summary of hydroxyl radical modification ratios for residues in the comparison of PT/PT-hT12 and PT-hT12/PT-hT72.

Residue number	Residue	Normalized modification ratio	Normalized modification ratio
		PT/PT-hT12	PT-hT12 /PT-hT72
POT1			
1	M	0.80	0.94
3	L	0.95	1.20
9	Y	0.99	1.21
10	I	0.83	1.29
18	K	0.81	1.82
22	I	0.70	1.29
36	Y	0.89	2.14
37	L	0.56	1.68
39	K	0.65	2.02
55	V	0.71	2.09
56	K	0.74	1.46
66	Y	3.03	1.69
71	I	0.74	1.08
73	Y	4.86	1.34
89	Y	0.71	1.55
90	K	0.71	1.55
91	K	0.73	1.66
110	L	1.07	1.30
113	P	0.86	0.64
115	I	0.72	0.95
121	K	1.02	0.47
122	Y	0.90	1.10
130	H	1.50	1.18
132	M	0.75	0.55
143	H	0.93	1.01
144	M	1.16	1.68
154	C	1.31	1.08
159	M	0.75	1.24
169	L	1.75	0.63
171	K	1.25	0.93
173	E	1.08	1.48
174	V	0.94	2.06
177	A	0.84	1.57
184	W	0.85	1.02
190	P	0.87	0.54
191	F	0.59	1.74
194	W	1.03	1.36
197	L	1.02	1.78
209	H	0.92	0.84
211	H	0.93	1.41
223	Y	0.87	2.07
228	H	1.46	1.64

Residue number	Residue	Normalized modification ratio	Normalized modification ratio
		PT/PT-hT12	PT-hT12 /PT-hT72
233	L	1.75	1.33
234	K	1.15	1.76
241	I	0.83	1.29
242	Y	9.74	0.72
251	M	0.71	1.23
266	H	6.65	0.20
271	Y	1.47	2.92
277	V	1.90	0.99
279	P	2.42	1.17
280	E	1.34	1.45
289	K	1.27	1.09
290	K	1.27	1.09
297	L	0.95	0.96
339	D	1.01	1.02
342	Y	0.96	1.17
354	Q	0.98	1.04
355	K	0.98	1.04
360	Y	0.91	1.79
369	Y	1.13	1.35
370	K	1.13	1.35
383	P	0.95	3.18
384	K	1.39	0.42
386	H	1.35	0.44
392	P	1.19	0.65
393	H	1.16	1.24
422	K	0.77	0.40
427	K	0.76	0.79
444	I	1.09	0.63
445	L	1.10	0.66
447	L	1.10	0.66
449	N	0.94	0.67
464	C	1.10	1.57
480	H	0.95	1.09
481	E	0.93	0.58
488	L	1.08	2.05
489	S	1.08	2.33
498	I	1.17	0.47
499	H	1.20	1.00
500	H	1.20	1.00
501	Y	1.30	0.66
518	L	1.02	1.21
519	V	0.83	1.85
533	L	0.87	1.63
536	V	1.16	0.84

Residue number	Residue	Normalized modification ratio	Normalized modification ratio
		PT/PT-hT12	PT-hT12 /PT-hT72
552	T	0.85	1.08
554	V	0.98	1.09
558	Y	0.88	0.73
560	M	0.86	1.23
567	Q	0.99	1.16
568	I	1.31	0.69
569	P	1.07	0.96
575	M	0.89	0.63
585	M	0.83	0.67
589	M	0.78	0.67
593	P	1.00	1.16
596	K	0.94	0.93
610	Y	1.13	0.69
619	Q	1.16	0.77
621	C	1.24	0.75
625	F	1.27	0.47
TPP1			
95	L	1.08	0.66
97	P	1.15	0.41
98	W	0.95	0.64
102	L	0.96	0.28
104	L	0.99	0.43
109	P	1.11	0.43
131	P	0.79	0.39
133	H	0.82	0.72
146	V	1.18	0.54
151	H	1.12	0.99
172	F	1.14	0.44

Residue number	Residue	Normalized modification ratio	Normalized modification ratio
		PT/PT-hT12	PT-hT12 /PT-hT72
202	F	1.35	0.60
203	Y	1.25	0.61
207	D	1.28	0.68
208	R	1.32	0.64
224	C	0.88	0.65
235	Y	1.04	0.40
237	C	1.16	0.85
261	M	0.52	0.92
267	H	0.89	1.77
281	L	0.97	0.69
284	P	0.81	0.83
285	C	0.90	1.14
288	P	0.83	0.53
292	H	0.93	0.72
298	C	1.50	0.10
312	M	0.79	0.81
321	L	0.95	0.95
322	I	0.89	0.91
328	P	0.96	1.02
329	C	0.87	0.64
331	R	1.01	0.70
*normalization factor		1.03	2.83
† mean-3SD		0.33	0.19
† mean-2SD		0.49	0.33
† mean		1.05	0.94
† mean+2SD		2.26	2.71
† mean+3SD		3.31	4.60

*The normalization factor is determined as the average of mean and median from all identified ratios of modification rates before normalization in log₁₀ scale, then converted back to linear scale.

† mean and SD are also calculated based on normalized modification rate ratios in log₁₀ scale, then mean±2SD and mean±3SD are determined, and finally converted back to linear scale.

References

1. Lei M, Podell ER, & Cech TR (2004) Structure of human POT1 bound to telomeric single-stranded DNA provides a model for chromosome end-protection. *Nature structural & molecular biology* 11(12):1223-1229.
2. Mullins MR, *et al.* (2016) POT1-TPP1 Binding and Unfolding of Telomere DNA Discriminates against Structural Polymorphism. *J Mol Biol* 428(13):2695-2708.
3. Xu G, Kiselar J, He Q, & Chance MR (2005) Secondary reactions and strategies to improve quantitative protein footprinting. *Analytical chemistry* 77(10):3029-3037.
4. Deperalta G, *et al.* (2013) Structural analysis of a therapeutic monoclonal antibody dimer by hydroxyl radical footprinting. *mAbs* 5(1):86-101.
5. van den Berg RA, Hoefsloot HC, Westerhuis JA, Smilde AK, & van der Werf MJ (2006) Centering, scaling, and transformations: improving the biological information content of metabolomics data. *BMC genomics* 7:142.
6. Wyatt PJ (1997) Multiangle light scattering: The basic tool for macromolecular characterization. *Instrum Sci Technol* 25(1):1-18.
7. Latrick CM & Cech TR (2010) POT1-TPP1 enhances telomerase processivity by slowing primer dissociation and aiding translocation. *The EMBO journal* 29(5):924-933.
8. Nandakumar J, *et al.* (2012) The TEL patch of telomere protein TPP1 mediates telomerase recruitment and processivity. *Nature* 492(7428):285-289.
9. Sentmanat MF, Peters ST, Florian CP, Connelly JP, & Pruett-Miller SM (2018) A Survey of Validation Strategies for CRISPR-Cas9 Editing. *Scientific reports* 8(1):888.
10. Harley CB, Futcher AB, & Greider CW (1990) Telomeres shorten during ageing of human fibroblasts. *Nature* 345(6274):458-460.
11. Wang F, *et al.* (2007) The POT1-TPP1 telomere complex is a telomerase processivity factor. *Nature* 445(7127):506-510.
12. Rice C, *et al.* (2017) Structural and functional analysis of the human POT1-TPP1 telomeric complex. *Nature communications* 8:14928.
13. Horvath MP, Schweiker VL, Bevilacqua JM, Ruggles JA, & Schultz SC (1998) Crystal structure of the Oxytricha nova telomere end binding protein complexed with single strand DNA. *Cell* 95(7):963-974.